

A Survey on Estimation Schemes in Molecular Communications

Xinyu Huang, Yuting Fang, and Nan Yang

Abstract—This survey paper focuses on the estimation schemes in molecular communications (MC) systems. The existing studies in estimation schemes can be divided into parameter estimation (e.g., distance, diffusion coefficient, and flow velocity) and channel estimation. In this paper, we present, for the first time, a comprehensive survey on i) distance estimation, since distance is the most widely estimated parameter in current studies, ii) estimation of other parameters (i.e. the parameters excluding distance), and iii) channel estimation that focuses on the channel impulse response (CIR). Moreover, we examine the noise that may impact on the estimation performance and the metrics applied to evaluate the performance of different estimation schemes. Numerical results are provided to compare the performance of different distance estimation schemes. In addition, future research directions in parameter estimation and channel estimation are identified and discussed.

Index Terms—Molecular communication, parameter estimation, channel estimation, survey.

I. INTRODUCTION

Molecular communications (MC) is an emerging technology in the past decade, which has great potential to facilitate nano-scale communication. Instead of using electromagnetic waves as information carriers as in the traditional wireless communication, MC uses small particles such as molecules or lipid vesicles to deliver information [1]. Moreover, MC owns unique merits such as biocompatibility and low energy consumption, which make MC more suitable for *in vivo* applications than other communication methods, e.g., electromagnetic methods.

Recently, some surveys and tutorials have discussed the benefits and challenges of MC from different perspectives, e.g., [1]–[5]. Specifically, [1] presented a detailed introduction on MC and provided an overall survey at the recent advances in the micro-scale MC and macro-scale MC. [2] presented a survey on the applications of MC and molecular networks with the focus of targeted drug delivery. [3] provided a tutorial review on mathematical channel modeling for diffusive MC systems. [4] reviewed the contributions to the architectures of transmitter (TX) and receiver (RX) among nanomaterial-based nanomachines and/or biological entities and provided a complete overview of modulation, coding, and detection techniques employed for MC. [5] provided a comprehensive review on mobile MC. Although these studies stand on their own merits, the estimation schemes in MC have yet to be reviewed and summarized.

X. Huang and N. Yang are with the School of Engineering, Australian National University, Canberra, ACT 2600, Australia (email: {xinyu.huang1, nan.yang}@anu.edu.au).

Y. Fang is with the Department of Electrical and Electronic Engineering, University of Melbourne, Parkville, VIC 2010, Australia (e-mail: yuting.fang@unimelb.edu.au).

The estimation schemes investigated in current studies can be classified into two categories, namely, parameter estimation and channel estimation. Estimated parameters usually include the distance between the TX and the RX, diffusion coefficient of information molecules (IMs), and the flow velocity in the MC environment. Among these parameters, distance estimation is the most popular research area in current studies. This is because that the distance between nanomachines is one of the most pivotal parameters for the communication channel. Specifically, we summarize the significance of distance estimation in MC systems as follows:

- Distance estimation can be adapted to improve the channel performance since the distance affects the transmission rate. If a TX obtains the knowledge about the distance, it can adjust the number of released molecules to achieve a high probability of molecules arriving at a RX and avoid using too many molecules to reduce interferences, such as inter-symbol interference (ISI) and interference with other channels.
- In the application of targeted drug delivery [2], it is highly important to know the accurate location of the target site, e.g., a tumor, in the human body such that drugs are delivered to this site. The target site can be localized by estimating the relative distance between the tumor and nanomachines [6].

It is noted that in biological systems, there exist some techniques to determine the distance between two nanomachines in MC. For example, a cell can estimate the relative distance from an organism via producing a type of molecules to establish a chemical gradient [7].

Apart from distance estimation, estimating other parameters (i.e. the parameters excluding the distance) is also essential for some promising MC applications. For example, the MC system can be deployed in a blood-vessel environment for the healthcare application. In this application, estimating the blood flow velocity can help to measure the blood pressure. Also, estimating the diffusion coefficients of IMs can help to determine the blood composition and identify major changes in blood cell counts [8]. Furthermore, estimating the degradation rate of IMs can help to measure the blood pH level since molecule degradation varies with the pH level [9, Ch. 10]. Motivated by these benefits, some studies, e.g., [10]–[12], have proposed different methods for parameter estimation.

Different from parameter estimation, channel estimation focuses on estimating the channel impulse response (CIR) in the MC system. Here, the CIR is defined as the probability of observing one IM at the RX at time t when an impulsive

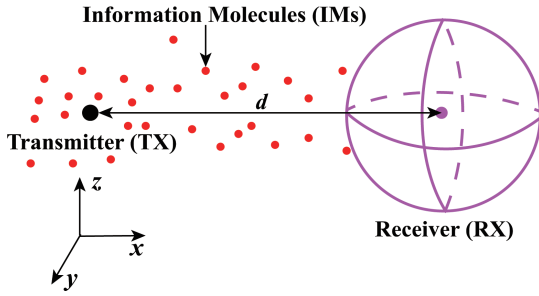


Fig. 1. Illustration of the MCvD environment where one point TX communicates with one spherical RX in a three-dimensional environment.

IMs is released at time $t_0 = 0$. The CIR is important for the design of equalization and detection schemes in MC systems [13], [14]. Motivated by this importance, a few studies has investigated the estimation of the CIR via different methods, e.g., [15], [16].

In this paper, we consider an MC via diffusion (MCvD) system and divide estimation schemes into three categories: Distance estimation, estimation of other parameters (i.e. the parameters excluding the distance), and channel estimation. For each category, we provide detailed reviews of current studies. In particular, our major contributions are summarized as follows:

- 1) We examine the noise that may affect the performance of an estimation scheme and the metrics that are usually used to assess the performance of an estimation scheme.
- 2) We provide a detailed review on different distance estimation schemes. Then we compare the performance of different methods via numerical results by calculating the mean squared error (MSE).
- 3) We divide other parameters into environmental parameters and channel performance governing parameters. Then we provide detailed reviews on each of them. Moreover, we review the pilot-based estimation scheme and the semi-blind CIR estimation scheme for channel estimation, and compare the performance of these two schemes.
- 4) We identify and discuss promising future research directions for parameter estimation and channel estimation.

The rest of this paper is organized as follows. In Section II, we introduce the MCvD environment and present a summary of the noise that may impact on the estimation performance. In Section III, we present metrics for evaluating the performance of an estimation scheme. In Section IV, we review the distance estimation schemes in current studies and compare the performance of different estimation schemes. In Section V, we review the estimation of other parameters. In Section VI, we review channel estimation. In Section VII, we present future research directions for parameter estimation and channel estimation. Conclusions are drawn in Section VIII.

II. MOLECULAR COMMUNICATION VIA DIFFUSION

We consider an MCvD system, as shown in Fig. 1, where one point TX communicates with one spherical RX with radius r_{RX} in an unbounded three-dimensional (3D) environment. The RX center is at a distance d away from the TX. We also

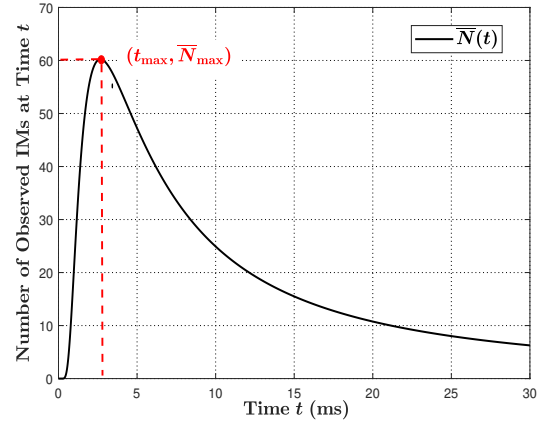


Fig. 2. The number of observed molecules within the transparent RX at time t versus time t , where $N_{\text{tx}} = 10^5$, $r_{\text{RX}} = 0.5 \mu\text{m}$, $d = 4 \mu\text{m}$, and $D = 1000 \mu\text{m}^2/\text{s}$ [19].

consider the TX as a point source which releases IMs into the environment.

A. Propagation Channel Modeling

We assume that the propagation channel outside the TX and the RX is filled with a fluid medium. Once IMs are released, they diffuse randomly in the propagation environment. The movement speed of IMs is determined by the diffusion coefficient, denoted by D , that is affected by the temperature of the fluid medium, the dynamic viscosity of the fluid, and the Stoke's radius of IMs. In this paper, we assume that the fluid medium has uniform temperature and viscosity such that D can be modeled as a constant value. It is noted that a more complex MC environment can incorporate flow with a constant velocity v and degradation of IMs, i.e., IMs of type A can degrade into some other molecular species \hat{A} with a constant degradation rate k . \hat{A} cannot be recognized by the RX.

B. Receiver Modeling

Current studies on estimation schemes focused on two types of RXs, i.e., transparent RX and fully-absorbing RX.

1) *Transparent RX Modeling:* The transparent RX does not impede the diffusion of IMs, nor interact with IMs. We count the number of free IMs that are within the RX volume as the received signal. We denote $h(t)$ as the CIR of the transparent RX, which is given by [17, eq. (4)]

$$h(t) = \frac{V_{\text{RX}}}{(4\pi D t)^{\frac{3}{2}}} \exp\left(-\frac{d^2}{4Dt}\right), \quad (1)$$

where V_{RX} is the volume of the RX and $V_{\text{RX}} = \frac{4}{3}\pi r_{\text{RX}}^3$ for the spherical RX. $h(t)$ that incorporates the flow and degradation of IMs is given by [13, eq. (13)]. It is noted that (1) is accurate when the RX is sufficiently far away from the TX, i.e., d is very large relative to r_{RX} . Thus, we can assume that the concentration of IMs at every point within the RX equals the concentration at the central point of the RX. If the RX is close to the TX, the uniform assumption of concentration does not hold. In this case, $h(t)$ is given by [18, eq. (47)].

We now denote $\bar{N}(t)$ as the expected number of IMs observed within the RX volume at time t . If an impulse of N_{tx} IMs is released from the TX at time $t_0 = 0$, $\bar{N}(t)$ is given by $\bar{N}(t) = N_{tx}h_t(t)$. In Fig. 2, we plot $\bar{N}(t)$ versus time t by adopting (1). From this figure, we observe a peak number of IMs observed within the RX. We denote the time for reaching the peak number of IMs observed as t_{max} . By taking the derivative of (1) with respective to t , t_{max} is calculated as [19, eq. (6)]

$$t_{max} = \frac{d^2}{6D}. \quad (2)$$

By substituting (2) into (1), we obtain the peak CIR, denoted by h_{max} , as

$$h_{max} = \left(d \sqrt{\frac{2\pi e}{3}} \right)^{-3} V_{RX}. \quad (3)$$

We denote \bar{N}_{max} as the expected peak number of IMs observed within the RX. Then \bar{N}_{max} is given by $\bar{N}_{max} = N_{tx}h_{max}$.

2) *Fully-Absorbing RX Modeling*: In biological systems, many practical RX surfaces may interact with the molecules of interest, e.g., by providing binding sites for absorption or other reactions [20]. Hence, the transparent RX model is oversimplified. One practical RX model is the fully-absorbing RX. In this model, the RX absorbs IMs as soon as they hit the surface. The fully-absorbing RX counts the total number of molecules absorbed as the received signal. We define the CIR of the fully-absorbing RX as the probability of absorption of one IM until time t , that is given by [21, eq. (23)].

C. Noise Modeling

We next review some factors that affect the performance of estimation and treat these factors as noise during the estimation process.

1) *Statistical Distribution of Received Signal*: Due to the random diffusion (RD) of IMs, the number of IMs observed at the RX is a random variable (RV) [22]. This randomness influences the performance of estimation. Due to the independent diffusion of IMs, any given molecule released by the TX is observed by the RX with a probability of $h(t)$. A binary state model applies and the number of IMs observed at time t , denoted by $N_{ob}(t)$, follows a binomial distribution with N_{tx} trials and success probability $h(t)$. This is mathematically expressed as

$$N_{ob}(t) \sim \mathcal{B}(N_{tx}, h(t)), \quad (4)$$

where $\mathcal{B}(N, p)$ represents a binomial distribution. Unfortunately, the binomial distribution is cumbersome to work with in MC systems. Therefore, current studies usually approximate binomial distribution as two distributions for the sake of mathematical tractability, described as follows:

(a) *Poisson distribution*: When the number of trials N_{tx} is large and the success probability $h(t)$ is small, $N_{ob}(t)$ can be approximated as a Poisson RV, given by

$$N_{ob}(t) \sim \mathcal{P}(N_{tx}h(t)), \quad (5)$$

where $\mathcal{P}(\varphi)$ represents the Poisson distribution with the mean of φ . Based on (5), the probability mass function (PMF) of the Poisson RV $N_{ob}(t)$ is written as

$$\Pr(N_{ob}(t) = \xi) = \frac{(N_{tx}h(t))^{\xi} \exp(-N_{tx}h(t))}{\xi!}, \quad (6)$$

where $\Pr(\cdot)$ stands for the probability.

(b) *Gaussian distribution*: If the expected number of IMs observed, i.e., $\bar{N}(t)$, is sufficiently large, we can apply the central limit theorem and approximate $N_{ob}(t)$ as a Gaussian RV, given by

$$N_{ob}(t) \sim \mathcal{N}(N_{tx}h(t), N_{tx}h(t)(1-h(t))). \quad (7)$$

The probability density function (PDF) of $N_{ob}(t)$ is given by

$$\Pr(N_{ob}(t) = \xi) = \frac{\exp\left(-\frac{(\xi - N_{tx}h(t))^2}{2N_{tx}h(t)(1-h(t))}\right)}{\sqrt{2\pi N_{tx}h(t)(1-h(t))}}. \quad (8)$$

2) *External Additive Noise*: In MC systems, the intended TX may not be the only source of IMs. Other sources, referred to as external sources, may also release the same type of IMs that influence the observation at the RX such that the estimation performance is affected. We detail some examples of external sources as follows:

(a) *Multiuser interference*: Noisy molecules are emitted by TXs in other MC systems.

(b) *Unintended leakage*: IMs can be leaked from membrane-bound containers, e.g., vesicles, within transceivers. A rupture can result in a steady or sudden release of IMs [23].

(c) *Output from unrelated biochemical processes*: Biocompatibility of the MC system may require the selection of naturally-occurring IMs. Therefore, other processes that produce the same type of IMs are noisy sources for the considered MC system. For example, calcium is commonly used as a messenger molecule within cellular systems [24, Ch. 16]. If calcium is applied as signaling molecules of the MC system in the biological environment, the naturally-occurring calcium would impact the MC system.

(d) *Unintended reception of other molecules*: Molecules that are highly similar to IMs may be recognized by the RX. For example, the receptors at the RX may bind to other molecules that have a very similar shape and size to IMs [24, Ch. 4].

We denote $N_{sig}(t)$ as the intended observed IMs and $n(t)$ as the observed noise molecules. Since intended IMs and noise molecules are indistinguishable, the total number of molecules observed at the RX at time t is given by

$$N_{ob}(t) = N_{sig}(t) + n(t). \quad (9)$$

The analysis of statistical distribution of $n(t)$ is built upon following assumptions:

A1) We denote \bar{n} as the expected number of noise molecules observed within the RX. We assume that \bar{n} is constant over the entire observation time.

A2) The observation of one noise molecule at the RX is independent of observations of other noise molecules.
A3) The uniform concentration assumption holds for noise molecules at the RX.

Based on A1)–A3), we model the number of observed noise molecules as a Poisson RV, due to the law of rare events (LRE) [25], i.e., $n(t) \sim \mathcal{P}(\bar{n})$.

3) *ISI*: This type of noise exists when the TX transmits multiple symbols to the RX. Due to the RD of IMs, the IMs from previously sent symbols may arrive at the RX in the current symbol interval, which influences the estimation in the current symbol interval.

III. PERFORMANCE METRICS FOR ESTIMATION SCHEMES

In this section, we review some metrics that are usually applied to evaluate the performance of an estimation scheme.

A. MSE

The MSE is usually applied to assess the quality of an estimation scheme. We denote θ as the unknown parameter and $\hat{\theta}$ as the estimated value of θ . The MSE of an estimation scheme is defined as [26]

$$\text{MSE}(\hat{\theta}) = \mathbb{E}[(\hat{\theta} - \theta)^2], \quad (10)$$

where $\mathbb{E}[\cdot]$ represents the expectation. The MSE can be written as the sum of the variance and squared bias of the estimation scheme, which is [27]

$$\text{MSE}(\hat{\theta}) = \text{Var}(\hat{\theta}) + \text{Bias}(\hat{\theta}, \theta)^2, \quad (11)$$

where the variance is $\text{Var}(\hat{\theta}) = \mathbb{E}[(\hat{\theta} - \mathbb{E}[\hat{\theta}])^2]$ and the squared bias is $\text{Bias}(\hat{\theta}, \theta)^2 = (\mathbb{E}[\hat{\theta}] - \theta)^2$. For any unbiased estimation scheme, $\mathbb{E}[\hat{\theta}] = \theta$. Thus, the MSE equals the variance.

B. Cramer-Rao Lower Bound (CRLB)

The CRLB is a lower bound on the variance of any unbiased estimation scheme [28, Ch. 3]. An estimation scheme is called the minimum-variance unbiased (MVU) estimator if its MSE of attains the CRLB. Therefore, the CRLB provides insights into the comparison of estimation schemes and the prediction of the performance of the MVU estimator.

1) *A Single Unknown Parameter*: We have an M -point data set $\mathbf{x} = [x_1, x_2, \dots, x_M]$ that depends on the unknown parameter θ . Hence, the data set \mathbf{x} will be applied to determine θ . To mathematically model the data set, we define a PDF as $p(\mathbf{x}; \theta)$ that is parameterized by the unknown parameter θ . For the CRLB to exist, the regularity condition must be satisfied, that is [28, Ch. 3]

$$\mathbb{E}\left[\frac{\partial \ln p(\mathbf{x}; \theta)}{\partial \theta}\right] = 0, \text{ for all } \theta \quad (12)$$

where the expectation is taken with respect to $p(\mathbf{x}; \theta)$. The CRLB of the variance of an unbiased estimation scheme is $\text{Var}(\hat{\theta}) \geq I^{-1}(\theta)$, where $I(\theta)$ is the Fisher information, given by [28, eq. (3.6)]

$$I(\theta) = -\mathbb{E}\left[\frac{\partial^2 \ln p(\mathbf{x}; \theta)}{\partial \theta^2}\right]. \quad (13)$$

2) *Multiple Unknown Parameters*: We now assume that the number of L parameters is unknown and define a vector that contains L number of unknown parameters as $\boldsymbol{\theta} = [\theta_1, \theta_2, \dots, \theta_L]$. We further define a PDF as $p(\mathbf{x}; \boldsymbol{\theta})$ that is parameterized by the unknown parameter vector $\boldsymbol{\theta}$. It is assumed that the PDF $p(\mathbf{x}; \boldsymbol{\theta})$ satisfies the regularity conditions, that is

$$\mathbb{E}\left[\frac{\partial \ln p(\mathbf{x}; \boldsymbol{\theta})}{\partial \boldsymbol{\theta}}\right] = \mathbf{0}, \text{ for all } \boldsymbol{\theta}, \quad (14)$$

where the expectation is taken with respect to $p(\mathbf{x}; \boldsymbol{\theta})$. We denote $\hat{\boldsymbol{\theta}}$ as the estimated parameter vector of $\boldsymbol{\theta}$. The covariance matrix of any unbiased estimation scheme $\hat{\boldsymbol{\theta}}$, denoted by $\mathbf{C}_{\hat{\boldsymbol{\theta}}}$, satisfies

$$\mathbf{C}_{\hat{\boldsymbol{\theta}}} - \mathbf{I}^{-1}(\boldsymbol{\theta}) \geq \mathbf{0}, \quad (15)$$

where $\mathbf{I}(\boldsymbol{\theta})$ is a $L \times L$ Fisher information matrix, given by

$$[\mathbf{I}(\boldsymbol{\theta})]_{ij} = -\mathbb{E}\left[\frac{\partial^2 \ln p(\mathbf{x}; \boldsymbol{\theta})}{\partial \theta_i \partial \theta_j}\right], \quad (16)$$

where $i = 1, 2, \dots, L$ and $j = 1, 2, \dots, L$. The derivatives are evaluated at the true value of $\boldsymbol{\theta}$. The CRLB of θ_i is found as the $[i, i]$ element of the inverse of $\mathbf{I}(\boldsymbol{\theta})$, which is

$$\text{Var}(\hat{\theta}_i) \geq [\mathbf{I}^{-1}(\boldsymbol{\theta})]_{ii}. \quad (17)$$

C. Hammersley-Chapman-Robbins Lower Bound (HCRLB)

The HCRLB is a lower bound on the variance of any unbiased estimation scheme for a function parameterized by the unknown parameter [29]. Compared to the CRLB, the HCRLB is tighter and does not need to satisfy the regularity condition, but the computation is more complex. We denote $g(\theta)$ as a function of the unknown parameter θ and $\hat{g}(\theta)$ as an estimated function of $g(\theta)$. The HCRLB on the variance of $\hat{g}(\theta)$ is given by

$$\text{Var}(\hat{g}(\theta)) \geq \sup_{\Delta} \frac{[g(\theta + \Delta) - g(\theta)]^2}{\mathbb{E}\left[\frac{p(\mathbf{x}; \theta + \Delta)}{p(\mathbf{x}; \theta)} - 1\right]^2}, \quad (18)$$

where \sup stands for supremum. In (18), the HCRLB converges to the CRLB when $\Delta \rightarrow 0$. The HCRLB can be applied to a wider range of problems. For example, if $p(\mathbf{x}; \theta)$ is non-differentiable, the Fisher information is not defined. Hence, the CRLB does not exist. However, the HCRLB may exist under this condition.

IV. DISTANCE ESTIMATION

In this section, we review the current studies on the estimation of the distance between the TX and the RX in MC systems. We classify the current studies about distance estimation into two-way estimation and one-way estimation in Section IV-A and Section IV-B, respectively. We summarize different distance estimation schemes in Table I. It is noted that some studies focused on the 1D environment while other studies focused on the 3D environment. To facilitate the comparison, we apply all estimation schemes in the 3D environment.

TABLE I
DISTANCE ESTIMATION SCHEMES FOR MC SYSTEMS

Name	References	Performance	Computational Complexity	Synchronization	Noise	TX Waveform	RX Type	Environment
RTT	[10], [30]	Moderate	Low	Not Required	RD	Impulse	Transparent	1D
SA	[10]	Low	Low	Not Required	RD	Impulse	Transparent	1D
Peak-based (One type of IM)	[31], [32]	Moderate	Low	Required	RD	Impulse	Transparent	1D, 2D
	[11]	Moderate	Low	Required	RD	Rectangular	Transparent	3D
	[33]	Moderate	Low	Required	RD	Impulse	Transparent	Cylindrical Ring-shaped Poiseuille flow
Peak-based (Two types of IMs)	[34], [35]	Low	Low	Not Required	RD	Impulse	Transparent	1D
ML	[19], [36]	High	High	Required	RD	Impulse	Transparent	3D, Flow IMs degradation
	[37]	High	High	Required	ISI, RD	Impulse	Transparent	3D
	[38]	High	High	Required	RD	Impulse	Transparent Diffusive	3D
Data Fitting	[39]	N/A	High	Required	RD	Impulse	Multiple Fully-absorbing	3D
Macro-scale	[40]	N/A	High	Required	N/A	Sprayer	MQ-3 Sensor	Tabletop

A. Two-Way Estimation

Two-way estimation schemes were proposed in [10] to estimate the distance between two transceivers that are labelled as T and R , respectively. Specifically, T first releases an impulse of IMs of type A at time t_0 . The diffusion coefficient of IMs A is D_A . When R detects the IMs A at time t_1 , it immediately transmits a feedback signal of an impulse of IMs B whose diffusion coefficient is D_B . At time t_2 , T detects the IMs B . T and R are regarded as transparent RXs when they detect IMs B and A , respectively.

1) *Round Trip Time (RTT) Protocols*: In RTT protocols, T measures the RTT that is the sum of time required for the transmission from T to R and for the transmission from R to T . The first estimation scheme is named as *RTT protocol from the peak concentration (RTT-P)*. In RTT-P, T transmits at time t_0 and R detects the peak concentration of IMs A from T at time t_1 . According to (2), we can obtain the relationship between $t_1 - t_0$ and d . T detects the peak concentration of the feedback signal with type B IMs at time t_2 . Similarly, we can obtain the relation between $t_2 - t_1$ and d based on (2). Accordingly, the distance d is estimated as a function of the RTT $t_2 - t_0$ as

$$\hat{d} = \sqrt{\frac{6D_A D_B}{D_A + D_B}(t_2 - t_0)}, \quad (19)$$

where \hat{d} is the estimated value of d .

The second estimation scheme was named as *RTT protocol from the threshold concentration (RTT-T)*. Different from RTT-P, RTT-T defines the threshold concentrations H_A and H_B for R and T to detect the number of IMs observed, respectively. It is assumed that T transmits N_{tx}^A number of IMs A and R transmits N_{tx}^B number of IMs B . R records t_1 when the number of molecules observed reach the threshold concentration H_A , i.e., $\bar{N}(t_1 - t_0)|_{D=D_A, N_{tx}=N_{tx}^A} = H_A$ by assuming $\bar{N}(t) = N_{ob}(t)$. Similarly, T records t_2 when the number of IMs observed reach the threshold concentration H_B , i.e., $\bar{N}(t_2 - t_1)|_{D=D_B, N_{tx}=N_{tx}^B} = H_B$. If $D_A = D_B$, $N_{tx}^A = N_{tx}^B$, and $H_A = H_B$, d is estimated as a function of

the RTT $t_2 - t_0$ as

$$\hat{d} = \sqrt{D_A(t_2 - t_0) \ln \left(\frac{V_{RX}^2 (N_{tx}^A)^2}{8\pi^3 D_A^3 H_A^2 (t_2 - t_0)^3} \right)}. \quad (20)$$

2) *Signal Attenuation Protocol from Peak Concentration (SA-P)*: In SA-P, T transmits type A IMs to R , and R measures the peak concentration, denoted by $N_{ob,m}^A$. According to (3), we can obtain the relationship between $N_{ob,m}^A$ and d . Similarly, R transmits type B of IMs and T measures the peak concentration, denoted by $N_{ob,m}^B$. By assuming $N_{tx}^B = N_{ob,m}^A$, \hat{d} is obtained as

$$\hat{d} = \sqrt{\frac{3}{2\pi e}} \left(\frac{N_{tx}^A V_{RX}^2}{N_{ob,m}^B} \right)^{\frac{1}{6}}. \quad (21)$$

The estimation performance of SA has been shown in [19].

3) *Merits and Drawbacks*: In this subsection, we summarize the merits and drawbacks of the two-way estimation. One merit of this method is that the synchronization between two transceivers is not required. For both RTT and SA protocols, only RTT, the number of emitted molecules, and peak concentration at T are required. Despite this merit, there are several drawbacks. The first drawback is that this method is time-consuming since it requires two-way transmission. The second one is that this method requires R to immediately send the feedback signal when it detects the type of IMs A , which is challenge for a nanomachine. The third drawback is that the instantaneous observation at the RX is used to approximate its expectation, which impacts on the estimation performance.

B. One-Way Estimation

Due to the aforementioned drawbacks of the two-way estimation, most current studies have focused on the acquisition of the distance information from the received signal only, referred to as one-way estimation.

1) *Peak-Based Estimation*: In this subsection, we review the studies that perform the estimation via measuring the peak received signal or the time for reaching the peak received signal.

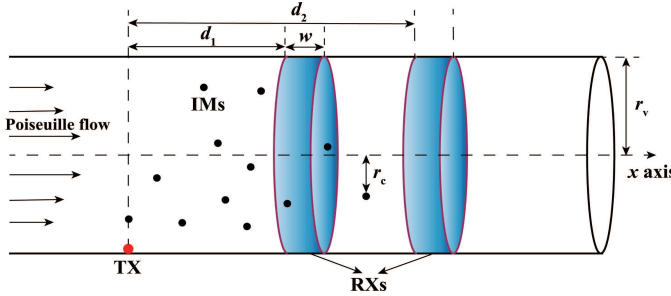


Fig. 3. Estimation in a cylindrical diffusive MC environment by using ring-shaped RXs; reproduced based on [33].

First, [31] performed the estimation based on the peak number of observed IMs, denoted by $N_{\text{ob,m}}$, at the transparent RX. According to (3), the distance d is estimated as

$$\hat{d} = \sqrt{\frac{3}{2\pi e}} \left(\frac{V_{\text{RX}} N_{\text{tx}}}{N_{\text{ob,m}}} \right)^{\frac{1}{3}}. \quad (22)$$

The estimation performance of this method is affected by the RD of IMs, since the instantaneous observation is used to approximate its expectation.

Second, [11] considered, for the first time, the release of IMs from the TX as a rectangular pulse which is given by

$$s(t) = A \text{rect} \left(\frac{t - \frac{T_e}{2}}{T_e} \right), \quad (23)$$

where T_e is the emission duration and $\text{rect}(\cdot)$ represents the rectangular function [41]. We denote $h_{\text{rec}}(t)$ as the CIR at the transparent RX when the TX releases the rectangular pulse. $h_{\text{rec}}(t)$ can be obtained as $h_{\text{rec}}(t) = s(t) * h(t)$. By taking the derivative of $h_{\text{rec}}(t)$ with respect to t , d can be estimated via measuring the time for reaching the peak concentration at the RX as

$$\hat{d} = \sqrt{\frac{6D t_{\text{max}} (t_{\text{max}} - T_e)}{T_e} \ln \left(\frac{t_{\text{max}}}{t_{\text{max}} - T_e} \right)}. \quad (24)$$

As t_{max} is involved in the estimation of [11], a perfect synchronization between the TX and the RX is required. [34], [35] proposed a low complexity scheme that does not require the synchronization via adopting two types of IMs. In this scheme, the TX releases type A IMs at time t_0 and the RX records the time of peak concentration of IMs A, denoted by t_{max}^A . Similarly, the TX transmits type B IMs at t_1 , and the RX records the time of peak concentration of IMs B, denoted by t_{max}^B . According to (2), the relation between t_{max}^A and d , and t_{max}^B and d are obtained. Thus, d is estimated as

$$\hat{d} = \sqrt{\frac{6D_A D_B (\Delta t_{\text{RX}} - \Delta t_{\text{TX}})}{D_A - D_B}}, \quad (25)$$

where $\Delta t_{\text{RX}} = t_{\text{max}}^B - t_{\text{max}}^A$ and $\Delta t_{\text{TX}} = t_1 - t_0$. We note that Δt_{RX} and Δt_{TX} are based on the time measurements at the RX and TX, respectively. Therefore, synchronization is not required.

In [10], [11], [31], [34], [35], estimation is performed in an unbounded environment. Different from these studies, [33] considered a cylindrical MC environment whose surface is

reflecting as shown in Fig. 3. Within the cylindrical environment, a point TX releases IMs into the environment and two ring-shaped RXs with a certain width w are located on the cylinder perimeter with a radius r_v that is the same as the cylinder's radius. After the IMs are released, they diffuse randomly with a constant diffusion coefficient D and subject to the Poiseuille flow [42]. As the cylindrical MC environment is a good approximation of the blood vessel environment, it has been widely investigated in current studies, e.g., [33], [43], [44]. Due to the existence of the Poiseuille flow, advection and diffusion can both transport IMs. The Péclet number [42, eq. (4.44)], denoted by Pe , is applied into evaluation if diffusion is more effective than advection or vice versa. If $\text{Pe} \ll 1$, diffusion dominates advection. If $\text{Pe} \gg 1$, advection dominates diffusion. [33] considered a diffusion-domain movement and only focused on the movement in the x axis, i.e., the channel is approximated as a 1D environment. [33] performed the estimation in two scenarios. The first scenario is that the emission time of IMs is known. By measuring the time of peak concentration, the distance can be estimated by a single RX as

$$\hat{d}_1 \approx \frac{-w + \sqrt{w^2 - 8(wv_m t_{\text{max}} - 2(v_m t_{\text{max}})^2 - 4D_e t_{\text{max}})}}{4}, \quad (26)$$

where $D_e = D (1 + \frac{1}{48} \text{Pe}^2)$ is the effective diffusion coefficient and $v_m = \frac{1}{2}(v_{\text{max}} + v_{\text{min}})$ is the average flow velocity. Here, v_{max} is the maximum flow velocity in the center of the cylinder, and $v_{\text{min}} = 0$ is the minimum flow velocity.

The second scenario is that the emission time is unknown. Thus, t_{max} is unknown and (26) contains two unknown parameters, i.e., d_1 and t_{max} . In this scenario, d_1 is estimated by using two RXs. Similar to (26), an equation containing d_1 and t_{max} can be obtained at the second RX. Thus, d_1 can be mathematically derived by jointly solving these two equations.

2) *Maximum Likelihood (ML) Estimation:* The ML distance estimation is to find \hat{d} that maximizes the joint observation likelihood. [19], [36] considered x_m , i.e., the m th data of the data set \mathbf{x} , as the number of IMs observed at the transparent RX at time t_m when IMs are released at time t_0 . It is assumed that each observation is independent and follows a Poisson distribution. Thus, $p(\mathbf{x}; \theta)$ is given by

$$p(\mathbf{x}; \theta) = \prod_{m=1}^M \frac{(N_{\text{tx}} h(t_m))^{x_m}}{x_m!} \exp(-N_{\text{tx}} h(t_m)). \quad (27)$$

Using (27), d is estimated by taking the partial derivative of $p(\mathbf{x}; \theta)$ with respect to d and setting it equal to 0. Moreover, [19] derived the CRLB for the variance of \hat{d} .

It is noted that [19], [36] only considered the transmission of one symbol from the TX to the RX. Different from that, [37] considered multiple symbols transmitted from the TX to the transparent RX, where ISI exists and may impact the estimation performance. Assuming that the RX makes one observation in each symbol interval, $p(\mathbf{x}; \theta)$ is the joint PDF of multiple observations. Based on $p(\mathbf{x}; \theta)$, d is estimated.

Previous studies have focused on the distance estimation in a static MC system where both TX and RX are static. Instead of that, [38] considered estimating the initial distance, i.e., the

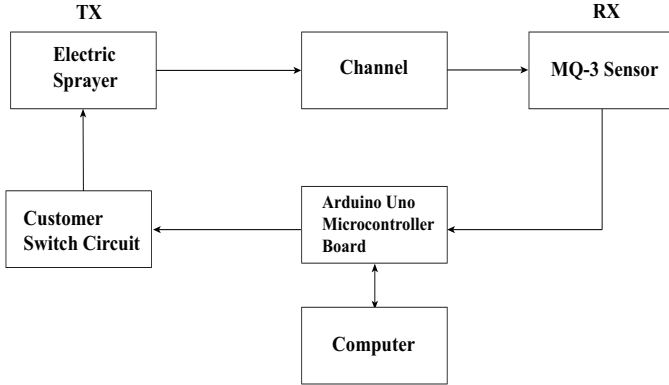


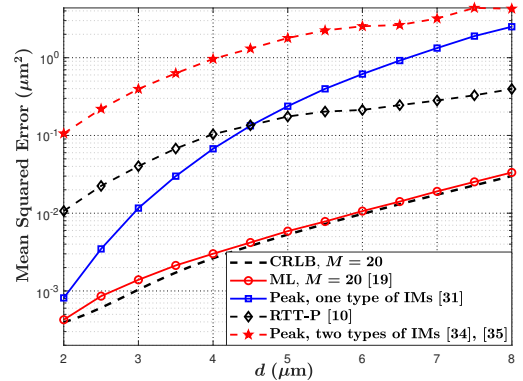
Fig. 4. Block diagram of the experimental setup in [40].

distance between the TX and the RX at the initial moment, in a diffusive mobile MC scenario, where both TX and RX diffuse with constant diffusion coefficients D_{TX} and D_{RX} , respectively. A novel two-step scheme is proposed to estimate the initial distance, denoted by d_0 . We denote $d(t)$ as the distance between the TX and the RX at time t , and the PDF of $d(t)$ is given by [38, eq. (13)]. Since d_0 is a parameter of the PDF of $d(t)$, d_0 can be estimated by the ML estimation for the joint PDF of M values of $d(t)$, that is $\mathbf{d} = [d(t_1), \dots, d(t_M)]$. Moreover, [38] proved that the ML estimation based on the joint PDF of \mathbf{d} can be simplified as performing the estimation based on the PDF of $d(t_1)$. Therefore, the first step is to estimate the stochastic distance $d(t_1)$, where the estimation scheme is similar to [19]. The second step is to estimate d_0 based on the estimated $\hat{d}(t_1)$. d_0 is estimated by finding \hat{d}_0 that maximizes the PDF of $d(t_1)$.

As the closed-form expression for \hat{d} is difficult to derive in the ML estimation, [37], [38] used the Newton-Raphson method, which is a method to find successively better approximations to the roots of a real-valued function, in order to calculate \hat{d} . The ML estimation scheme usually achieves high accuracy, but requires a high computational complexity and a perfect synchronization between the TX and the RX.

3) *Multiple Non-transparent RXs*: Previous studies have performed the estimation in an environment with a single RX or multiple transparent RXs. However, the estimation in an environment with multiple non-transparent RXs has not yet been investigated. Due to the fact that one non-transparent RX would impact IMs received by other non-transparent RXs, an accurate characterization of such dependence makes the estimation cumbersome. [39] performed the estimation in an environment with multiple fully-absorbing RXs. Due to the difficulty of deriving the number of IMs absorbed at each RX, [39] adopted the curve fitting method to obtain the expression for the number of absorbed IMs. Specifically, [39] used the nonlinear least squares method for curve fitting to obtain the distance, where the Levenberg-Marquardt (LM) method [45] is adopted.

4) *Macro-scale MC Systems*: Previous studies have focused on the distance estimation in micro-scale (nm to μm) MC systems. With this focus, these studies have considered an ideal channel model where the transmitted molecules do not have an initial velocity, the IMs move according to Brownian

Fig. 5. The MSE of different estimation schemes versus d .

motion, and the TX and the RX perfectly transmits and receives signals, respectively. In nature, MC also exists in the macro-scale (cm to m) environment. For example, animals like bees, flies, and ants use pheromone to send messengers over several meters. Against this background, [40] investigated, for the first time, the distance estimation in the macro-scale environment. Instead of analyzing in a theoretical model, [40] established an experimental setup similar to the tabletop platform in [46]. Fig. 4 shows the block diagram of the experimental setup. The TX is an electric sprayer controlled by a micro-controller via a custom switch circuit to release ethyl alcohol molecules. The RX receives the molecular signal with an MQ-3 alcohol sensor. The TX and the RX are both controlled by an Arduino Uno micro-controller board which is connected to a computer. Five different practical methods were proposed for distance estimation at the RX. The first two methods adopt the supervised machine learning, where multivariate linear regression and neural network regression are used as machine learning methods. These methods use the extracted features, e.g., rise time on the rising edge of the measured signal, from the received molecular signals as inputs. The other three methods analyze the collected data, which are less complex but less accurate than machine learning methods. The first data analysis method employs the received power to estimate the distance. The second data analysis method employs the peak time of the received signal. The third method combines the power and peak time of the received signal to estimate the distance.

C. Performance Comparison

In this subsection, we present numerical results to compare the distance estimation performance of different estimation schemes via calculating their MSE. Particle-based simulation is used to simulate the random propagation of IMs [47]. The simulation time step is $\Delta t_{\text{sim}} = 0.0001$ s and all results are averaged over 10,000 realizations. Throughout this subsection, we set $N_{\text{tx}} = N_{\text{tx}}^A = N_{\text{tx}}^B = 10^5$, $r_{\text{R}} = 0.5 \mu\text{m}$, $D = D_A = 1000 \mu\text{m}^2/\text{s}$, and $D_B = 500 \mu\text{m}^2/\text{s}$ [12].

In Fig. 5, we plot the MSE of different estimation schemes versus the distance d . Here, estimation schemes include the RTT-P [10], the ML estimation [19], the peak-based estimation for applying a single type of IMs [31] and two types of IMs [34], [35]. We also plot the CRLB as a lower bound to assess

TABLE II
PARAMETER ESTIMATION SCHEMES FOR MC SYSTEMS

Name	Estimated Parameter	Reference	Method	Noise	TX Waveform	RX Type	Environment
Environmental Parameters	d, t_0, D, v, k, N_{tx}	[12]	ML	RD	Impulse	Transparent	3D, flow, IMs degradation
	N_{tx}	[48]	HCRLB	RD, ISI	Impulse	Transparent	3D
	D	[49]	Transfer Function	RD	Continuous	Two Fully-absorbing	1D
	d, v, k	[50]	Method of Moments	RD, External	Continuous	Two Fully-absorbing	1D, flow, IMs degradation
Channel Performance Governing Parameters	Clock Offset	[51]	ML	RD	Impulse	Transparent	1D
	SNR	[52]	ML	ISI, RD	Impulse	Transparent	3D

the performance of each estimation scheme. For the CRLB and ML estimation, we apply $M = 20$ observations. First, we observe that the MSE of ML estimation almost attains the CRLB and hence achieves the best performance. Second, we observe that the peak-based estimation using one type of IMs and RTT-P achieves a moderate performance. The peak-based estimation using one type of IMs outperforms the RTT-P when d is small. When d is large, the advantage of RTT-P becomes more obvious. Third, the peak-based estimation using two types of IMs achieves the worst performance since it calculates the time difference, but does not need the synchronization.

V. ESTIMATION OF OTHER PARAMETERS

In this section, we review the current studies on the estimation of other parameters (i.e. the parameters excluding distance). We classify these parameters into two categories. The first category is referred to as the *environmental parameters* that are related to channel and TX properties, e.g., diffusion coefficient and the number of released molecules. The second category is referred to as the *channel performance governing parameters* that include the signal-to-noise ratio (SNR) and time offset between the TX and the RX. We summarize the studies that estimate other parameters in Table II.

A. Environmental Parameters

In this subsection, we focus on the studies on the estimation of environmental parameters. Specifically, environmental parameters include the distance between the TX and the RX, release time of IMs, diffusion coefficient of IMs, degradation rate of IMs, flow velocity, and the number of released IMs.

[12] considered a joint environmental parameter estimation, where the unknown parameter vector θ contains a single or multiple parameters. By assuming each observation of the received signal at the transparent RX is independent and follows a Poisson distribution, the joint PMF of M observations is given by

$$p(\mathbf{x}; \theta) = \prod_{m=1}^M \frac{(N_{tx} h_t(t_m))^{x_m}}{x_m!} \exp(-N_{tx} h_t(t_m)). \quad (28)$$

Based on (28), [12] derived the Fisher information matrix $\mathbf{I}(\theta)$ and the CRLB when a single unknown parameter exists or multiple unknown parameters exist. Moreover, the ML estimation was applied to estimate the unknown parameters.

[48] evaluated the HCRLB for a special case via setting $g(\theta) = N_{tx}$, i.e., the HCRLB for the variance of the estimated number of released IMs was derived. Similar to (27), [48] derived $p(\mathbf{x}; \theta)$ as the joint PMF of the received signals at the transparent RX.

It is noted that [12], [48] investigated parameter estimation for a single RX only. Based on these studies, [49], [50] investigated parameter estimation for two fully-absorbing RXs in a 1D environment. [49] applied the transfer function to estimate the diffusion coefficient of IMs. Compared to the previous studies, [50] considered, for the first time, the existence of the external additive noise in the parameter estimation process. To reduce the impact of the external additive noise, [50] proposed a novel estimation scheme – difference estimation (DE) – to estimate the unknown parameter based on the difference between received signals at two RXs. According to the CIR derived between the TX and each fully-absorbing RX in [53, eq. (8)], [50] derived the CRLB on the variance of the unknown parameter. By assuming that each observation of the received signal is independent and follows a Poisson distribution, $p(\mathbf{x}; \theta)$ was obtained as the joint PMF for the difference of received signals at two RX. In addition, [50] applied the method of moments [28, Ch.9] to estimate the unknown parameter.

B. Channel Performance Governing Parameters

In this subsection, we review the studies on the estimation of channel performance governing parameters. These parameters include the clock offset between the TX and the RX and the SNR. The clock offset describes a time difference between the TX and the RX. In a nanonetwork system, different nanomachines work based on their own clocks. Thus, estimating the clock offset is crucial to establish a reliable communication link between synchronized TX and RX.

[51] estimated the clock offset between two transceivers, denoted by T and R , respectively, via proposing a two-way message exchange mechanism. In the ε th round of the message exchange, T sends IMs at time $T_{1,\varepsilon}$, and R receives the message at time $T_{2,\varepsilon}$. R then sends a feedback signal at time $T_{3,\varepsilon}$, and T receives the signal at time $T_{4,\varepsilon}$. After α rounds of message exchange, T obtains a set of time instants $\{T_{1,\varepsilon}, T_{2,\varepsilon}, T_{3,\varepsilon}, T_{4,\varepsilon}\}_{\varepsilon=1}^{\alpha}$. Thus, the joint PDF of the molecular propagation delay for the α -round message exchange can be obtained. Based on the PDF, the clock offset is estimated

via the ML estimation. After that, R can be synchronized to T .

[52] estimated the SNR in the MC system, which considered the noise induced by the ISI. In [52], the SNR was defined as

$$\text{SNR} = \frac{P_s}{P_n}, \quad (29)$$

where P_s represents the power of the intended received signal at the transparent RX and P_n represents the power of noise due to the ISI. The power in MC can be interpreted as the square number of IMs. Thus, the SNR is a function of the number of emitted IMs N_{tx} and the variance of the noise, denoted by σ_n^2 , where the noise is regarded as a Gaussian RV. According to the invariance property of the ML estimation, estimating a function with multiple unknown parameters is equivalent to estimating individual unknown parameters [28]. Therefore, the SNR is estimated by using the ML estimation of N_{tx} and σ_n^2 based on the joint PDF of the received signals at the RX. In addition, the CRLB was derived when $\theta = [N_{\text{tx}}^2, \sigma_n^2]$.

VI. CHANNEL ESTIMATION

In this section, we first present the CIR estimation problem and then review different CIR estimation schemes.

A. Problem Formulation

We consider an MC system as shown in Fig. 1. At the beginning of each symbol interval, the TX releases N_{tx} IMs if the transmitted symbol is “1”, but does not release any IM if the transmitted symbol is “0”. Taking into account the effect of ISI, we assume the input-output relationship of the MC system as

$$z[q] = \sum_{u=1}^U c_u[q] + c_n[q], \quad (30)$$

where $z[q]$ is the number of IMs detected at the RX in symbol interval q , U is the number of memory taps of the channel, and $c_u[q]$ is the number of IMs observed at the RX in symbol interval u , due to the release of $b[q-u+1]N_{\text{tx}}$ IMs by the TX in symbol interval $q-u+1$, where $b[q] \in [0, 1]$ is the transmitted symbol in symbol interval q . Therefore, $c_u[q]$ can be well approximated by a Poisson RV with the mean of $\bar{c}_u b[q-u+1]$. Moreover, $c_n[q]$ is the number of external additive noise molecules detected by the RX in the symbol interval q . Let $\mathbf{b} = [b[1], b[2], \dots, b[Q]]^T$ be a training sequence of length Q .

For convenience of notation, we define $\mathbf{z} = [z[U], z[U+1], \dots, z[Q]]^T$, $\bar{\mathbf{c}} = [\bar{c}_1, \bar{c}_2, \dots, \bar{c}_U, \bar{c}_n]^T$ is the CIR of the channel, and $f_{\mathbf{z}}(\mathbf{z}|\bar{\mathbf{c}}, \mathbf{b})$ is the PDF of the observation \mathbf{z} conditioned on a given channel $\bar{\mathbf{c}}$ and a given training sequence \mathbf{b} . The goal of channel estimation is to estimate $\bar{\mathbf{c}}$ based on the vector of random observations \mathbf{z} .

B. Pilot-Based CIR Estimation

In this subsection, we present the pilot-based CIR estimation scheme studied in [15], where the transmission of a known training sequence of pilots is required for estimation and the corresponding CRLB.

Algorithm 1 ML (or LSSE) CIR estimation of $\hat{\mathbf{c}}^{\text{ML}}$ (or $\hat{\mathbf{c}}^{\text{LSSE}}$) [15]

```

initialize  $\mathcal{A}_w = \mathcal{F}$  and solve (33) (or (35)) to find  $\bar{\mathbf{c}}^{\mathcal{F}}$ 
if  $\bar{\mathbf{c}}^{\mathcal{F}} \geq \mathbf{0}$  then
    Set  $\hat{\mathbf{c}}^{\text{ML}} = \bar{\mathbf{c}}^{\mathcal{F}}$  (or  $\hat{\mathbf{c}}^{\text{LSSE}} = \bar{\mathbf{c}}^{\mathcal{F}}$ )
else
    for  $\forall \mathcal{A}_w \neq \mathcal{F}$  do
        Solve (33) (or (35)) to find  $\bar{\mathbf{c}}^{\mathcal{A}_w}$ 
        if  $\bar{\mathbf{c}}^{\mathcal{A}_w} \geq \mathbf{0}$  holds then
            Set the values of the elements of  $\hat{\mathbf{c}}^{\text{CAN}}$ , whose
            indices are in  $\mathcal{A}_w$ , equal to the values of the corresponding
            elements in  $\bar{\mathbf{c}}^{\mathcal{A}_w}$  and the remaining  $U + 1 - |\mathcal{A}_w|$  elements
            equal to zero;
            Save  $\hat{\mathbf{c}}^{\text{CAN}}$  in the candidate set  $\mathcal{C}$ 
        else
            Discard  $\bar{\mathbf{c}}^{\mathcal{A}_w}$ 
        end if
    end for
    Choose  $\hat{\mathbf{c}}^{\text{ML}}$  (or  $\hat{\mathbf{c}}^{\text{LSSE}}$ ) equal to  $\hat{\mathbf{c}}^{\text{CAN}}$  in the candidate set
     $\mathcal{C}$  which maximizes  $g(\bar{\mathbf{c}})$  (or minimizes  $\|\mathbf{e}\|^2$ ).
end if

```

1) *ML Estimation*: The ML CIR estimation scheme aims to find the CIR that maximizes the likelihood of observation vector \mathbf{z} [54]. In particular, the ML estimation is given by

$$\hat{\mathbf{c}}^{\text{ML}} = \underset{\bar{\mathbf{c}} \geq \mathbf{0}}{\text{argmax}} f_{\mathbf{z}}(\mathbf{z}|\bar{\mathbf{c}}, \mathbf{b}). \quad (31)$$

We assume that $z[q]$ is a Poisson RV with the mean of $\bar{z}[q] = \bar{c}_n + \sum_{u=1}^U \bar{c}_u b[q-u+1] = \bar{\mathbf{c}}^T \mathbf{b}_q$ and $\mathbf{b}_q = [b[q], b[q-1], \dots, b[q-U+1], 1]^T$. Under this assumption, $f_{\mathbf{z}}(\mathbf{z}|\bar{\mathbf{c}}, \mathbf{b})$ is given by

$$f_{\mathbf{z}}(\mathbf{z}|\bar{\mathbf{c}}, \mathbf{b}) = \prod_{q=U}^Q \frac{(\bar{\mathbf{c}}^T \mathbf{b}_q)^{z[q]}}{z[q]!} \exp(-\bar{\mathbf{c}}^T \mathbf{b}_q). \quad (32)$$

We note that [15] solved the ML estimation of the CIR given in (31) by using **Algorithm 1**, where the following non-linear system of equations is solved¹ for different \mathcal{A}_n

$$\sum_{q=L}^Q \left[\frac{z[q]}{(\bar{\mathbf{c}}^{\mathcal{A}_w})^T \mathbf{b}_q^{\mathcal{A}_w}} - 1 \right] \mathbf{b}_q^{\mathcal{A}_w} = \mathbf{0}, \quad (33)$$

where $\mathcal{A} = \{\mathcal{A}_1, \mathcal{A}_2, \dots, \mathcal{A}_W\}$ denotes a set which contains all possible $W = 2^{U+1} - 1$ subsets of the set $\mathcal{F} = \{1, 2, \dots, U, n\}$, except for the empty set. Here, \mathcal{A}_w denotes the w -th subset of \mathcal{A} , $w = 1, 2, \dots, W$. Moreover, let $\bar{\mathbf{c}}^{\mathcal{A}_w}$ and $\mathbf{b}_q^{\mathcal{A}_w}$ denote the reduced-dimension versions of $\bar{\mathbf{c}}$ and \mathbf{b}_q , respectively, which only contain those elements of $\bar{\mathbf{c}}$ and \mathbf{b}_q whose indices are the elements of \mathcal{A}_w , respectively.

2) *Least Sum of Squared Errors (LSSE) CIR Estimation*: The LSSE CIR estimation scheme aims to choose $\bar{\mathbf{c}}$ that minimizes the sum of the squared errors for the observation vector \mathbf{z} . Here, the error vector is defined as $\mathbf{e} = \mathbf{z} - \mathbb{E}\{\mathbf{z}\} = \mathbf{z} - \mathbf{B}\bar{\mathbf{c}}$

¹A system of nonlinear equations can be solved by using mathematical software packages, e.g., Mathematica.

where $\mathbf{B} = [\mathbf{b}_U, \mathbf{b}_{U+1}, \dots, \mathbf{b}_Q]^T$. In particular, the LSSE CIR estimation can be written as

$$\hat{\mathbf{c}}^{\text{LSSE}} = \underset{\mathbf{\bar{c}} \geq \mathbf{0}}{\operatorname{argmin}} \|\mathbf{e}\|^2. \quad (34)$$

It is noted that [15] also obtained the LSSE estimation of the CIR by solving (34). The solution is given by **Algorithm 1** where for a given set \mathcal{A}_w , $\bar{\mathbf{c}}^{\mathcal{A}_w}$ is obtained as

$$\bar{\mathbf{c}}^{\mathcal{A}_w} = ((\mathbf{B}^{\mathcal{A}_w})^T \mathbf{B}^{\mathcal{A}_w})^{-1} (\mathbf{B}^{\mathcal{A}_w})^T \mathbf{z}. \quad (35)$$

3) *CRLB*: With the estimation error vector defined as $\mathbf{e} = \bar{\mathbf{c}} - \hat{\mathbf{c}}$, the classical CRLB for the deterministic $\bar{\mathbf{c}}$ provides the following lower bound on the sum of the expected square errors [15]

$$\mathbb{E}\{\|\mathbf{e}\|^2\} \geq \operatorname{tr}\{\mathbf{I}^{-1}(\bar{\mathbf{c}})\} = \operatorname{tr}\left\{\left[\sum_{q=U}^Q \frac{\mathbf{b}_q \mathbf{b}_q^T}{\bar{\mathbf{c}}^T \mathbf{b}_q}\right]^{-1}\right\}, \quad (36)$$

where tr denotes the trace of a matrix. While [15] derived the ML and LSSE estimation schemes of the CIR and the CRLB for a single-input single-output channel, [16] extended these results to a diffusive multiple-input multiple-output (MIMO) system, by incorporating the inter-link interference.

C. Semi-Blind CIR Estimation

In this subsection, we present semi-blind CIR estimation schemes where the transmission of Q pilot symbols is followed by the transmission of \mathcal{D} unknown data symbols, denoted by the vector $\beta = [\beta[1], \beta[2], \dots, \beta[\mathcal{D}]]^T$. The semi-blind CIR estimation schemes incorporate both data-carrying and pilot-carrying observations into the estimation process. This is different from pilot-based estimation which only considers the received pilot-carrying observations in the estimation process but excludes data-carrying observations. Incorporating data-carrying observations into the estimation can significantly enhance the estimation accuracy and/or improve the data rate [55].

An expectation maximization (EM)-based estimation scheme was first proposed in [55]. The data vector β constitutes hidden information at the RX. Beginning with an initial guess, the EM estimation scheme alternates between obtaining the conditional expectation of the complete-data log-likelihood and maximizing the result with respect to the desired parameters. The ε th iteration of the EM estimation scheme consists of two steps. The first is the expectation step (E-step) which consists of obtaining the expectation of the complete-data log-likelihood function. This is followed by the maximization step (M-step), in which the *posterior* probability of the hidden data is maximized to acquire an updated estimate of CIR. [55] also proposed other two semi-blind estimation schemes based on the decision-directed (DD) strategy. The idea of DD strategy is to use the channel estimate acquired through pilot-based estimation for performing data detection. The detected data is in turn treated as a new set of pilots to perform another cycle of channel estimation [55]. We note that the analytical derivation of the CRLB can be very challenging in semi-blind estimation, because the log-likelihood function

of the observations becomes complicated when the statistics of the data symbols are taken into account. [55] applied the Monte-Carlo method to obtain accurate approximations of the Fisher information matrix $\mathbf{I}^{-1}(\bar{\mathbf{c}})$. The semi-blind CRLB was then obtained by evaluating $\operatorname{tr}\{\mathbf{I}^{-1}(\bar{\mathbf{c}})\}$.

D. Pilot-Based Estimation versus Semi-Blind Estimation

Based on the simulation results in [55], the semi-blind estimation schemes achieve a significantly lower MSE than the existing pilot-based ML and LSSE estimation schemes. Also, the semi-blind estimation schemes can substantially reduce the pilot overhead as compared to the best-performing pilot-based estimation schemes, by more than 60% for the case of EM and 55%–44% for DD-based estimation. The EM-based semi-blind estimation scheme provides the highest estimation accuracy. The DD-based semi-blind estimation scheme performs almost midway between the pilot-based ML and the EM-based semi-blind estimation schemes, but achieves a lower computational cost than the EM-based semi-blind estimation scheme.

VII. FUTURE RESEARCH DIRECTIONS

In this section, we identify and discuss some future research directions for parameter estimation and channel estimation in the MC system. Current studies on estimation have usually considered simple TX and RX protocols and ideal communication channels. These simplifications would lead to inaccuracy when the current estimation schemes are applied into practical MC environments. Moreover, the external additive noise is common in MC systems. Effective methods to mitigate the impact of the external noise on the estimation performance needs to be widely investigated. Based on these, we present some open research problems as follows:

- **Reactive RX:** Most studies on estimation schemes have considered the transparent RX, while some of them have considered the fully-absorbing RX. Compared to these two types of RXs, reactive RX is a more practical RX model, whose surface receptors reversibly react with IMs [56]. Incorporating the reactive RX into estimation schemes has not yet been investigated.
- **Imperfect TX:** Current studies on estimation schemes have considered an ideal point TX. Compared to realistic scenarios, this ideal TX model does not address the properties of the TX, such as geometry, signaling pathways inside the TX, and chemical reactions during the release process. Some recent studies have proposed imperfect TX models, e.g., an ion channel-based TX in [57] and a membrane fusion-based TX in [58]. Applying these imperfect TX into estimation schemes is an interesting future work.
- **Macro-scale estimation:** Most current studies have examined the estimation in the micro-scale environment while a few studies have considered macro-scale estimation. As aforementioned, MC also exists in macro-scale. Thus, the estimation in the micro-scale environment needs attention. Here, we propose two research directions. The first direction is to perform estimation

based on tabletop experiments. Some studies have established the tabletop experiment for macro-scale MC, e.g., [46], [59], [60]. Estimation can be investigated based on these experiments. The second direction is the theoretical analysis of estimation performance in practical macro-scale environments, e.g., a pipe or river. Compared to traditional theoretical analysis in micro-scale MC, flow modeling is crucial for the analysis in the macro-scale environment. For example, the flow can be modeled as laminar in the pipe and turbulent in the river.

- **Noise mitigation:** Most studies have considered noise induced by the RD of IMs and some studies have also considered ISI. Currently, only [50] considered the impact of external additive noise on the estimation. Despite so, [50] focused on a stable stage of the communication channel, i.e., the expected received signal is constant, when time is large. The impact of external noise on the estimation in an unstable stage has not yet been investigated and effective methods to mitigate the impact of external noise also need to be designed.
- **Multiple-RX estimation:** Most of existing studies have focused on estimation via one TX and one RX. Only a limited number of studies, such as [50], investigated cooperative estimation via two RXs and showed the improved estimation accuracy as compared to the single-RX estimation. Meanwhile, a few studies, such as [61], showed that the detection performance of transmitted symbols is greatly improved by combining the received information at multiple distributed receivers. Based on these studies, the performance enhancement in parameter or channel estimation by combining the received information at multiple receivers has not been thoroughly explored yet.
- **Real-time parameter estimation:** The existing studies have focused on one-shot parameter estimation by assuming that the estimated parameters are constant over time, or have focused on the estimation of the initial value of parameters when the estimated parameters keep changing over time. However, in dynamic biological environments, many parameters vary over time, e.g., the distance between the TX and RX changes when the transceivers move. Hence, the real-time estimation of time-varying parameters is a promising research direction.

VIII. CONCLUSION

In this paper, we provided the first comprehensive survey on parameter estimation and channel estimation in MC systems. We considered an MCvD environment and summarized three types of noise that can influence the estimation performance. We also summarized three metrics that can be used to evaluate the performance of an estimation scheme. For parameter estimation, we first presented a detailed review on the distance estimation and compare the performance of different estimation schemes via calculating the MSE. We then provided a detailed review on the estimation of other parameters. For channel estimation, we reviewed the pilot-based CIR estimation scheme and the semi-blind CIR estimation

scheme. Finally, we discussed some open research problems for parameter estimation and channel estimation. This survey helps MC researchers to develop an in-depth understanding on the current estimation schemes in MC and serves as a cornerstone for MC researchers to explore more advanced estimation schemes in the future.

REFERENCES

- [1] N. Farsad, H. B. Yilmaz, A. Eckford, C.-B. Chae, and W. Guo, “A comprehensive survey of recent advancements in molecular communication,” *IEEE Commun. Surv. Tut.*, vol. 18, no. 3, pp. 1887–1919, 3rd Quarter 2016.
- [2] U. A. Chude-Okonkwo, R. Malekian, B. T. Maharaj, and A. V. Vasilakos, “Molecular communication and nanonetwork for targeted drug delivery: A survey,” *IEEE Commun. Surv. Tut.*, vol. 19, no. 4, pp. 3046–3096, 4th Quarter 2017.
- [3] V. Jamali, A. Ahmadzadeh, W. Wicke, A. Noel, and R. Schober, “Channel modeling for diffusive molecular communication—a tutorial review,” *Proc. IEEE*, vol. 107, no. 7, pp. 1256–1301, Jul. 2019.
- [4] M. Kuscu, E. Dinc, B. A. Bilgin, H. Ramezani, and O. B. Akan, “Transmitter and receiver architectures for molecular communications: A survey on physical design with modulation, coding, and detection techniques,” *Proc. IEEE*, vol. 107, no. 7, pp. 1302–1341, Jul. 2019.
- [5] T. Nakano, Y. Okaie, S. Kobayashi, T. Hara, Y. Hiraoka, and T. Haraguchi, “Methods and applications of mobile molecular communication,” *Proc. IEEE*, vol. 107, no. 7, pp. 1442–1456, Jul. 2019.
- [6] M. J. Moore and T. Nakano, “Addressing by beacon distances using molecular communication,” *Nano Commun. Netw.*, vol. 2, no. 2-3, pp. 161–173, 2011.
- [7] F. Tostevin, P. R. Ten Wolde, and M. Howard, “Fundamental limits to position determination by concentration gradients,” *PLoS Comput. Biol.*, vol. 3, no. 4, pp. 763–771, Apr. 2007.
- [8] C.-H. Ho, “White blood cell and platelet counts could affect whole blood viscosity,” *J. Chin. Med. Assoc.*, vol. 67, no. 8, pp. 394–397, Aug. 2004.
- [9] R. Chang, *Physical Chemistry for the Biosciences*. Sausalito, CA, USA: Univ. Science Books, 2005.
- [10] M. J. Moore, T. Nakano, A. Enomoto, and T. Suda, “Measuring distance from single spike feedback signals in molecular communication,” *IEEE Trans. Signal Process.*, vol. 60, no. 7, pp. 3576–3587, Jul. 2012.
- [11] X. Wang, M. D. Higgins, and M. S. Leeson, “Distance estimation schemes for diffusion based molecular communication systems,” *IEEE Commun. Lett.*, vol. 19, no. 3, pp. 399–402, Mar. 2015.
- [12] A. Noel, K. C. Cheung, and R. Schober, “Joint channel parameter estimation via diffusive molecular communication,” *IEEE Trans. Mol. Biol. Multi-Scale Commun.*, vol. 1, no. 1, pp. 4–17, Mar. 2015.
- [13] —, “Optimal receiver design for diffusive molecular communication with flow and additive noise,” *IEEE Trans. Nanobiosci.*, vol. 13, no. 3, pp. 350–362, Sep. 2014.
- [14] M. U. Mahfuz, D. Makrakis, and H. T. Mouftah, “A comprehensive study of sampling-based optimum signal detection in concentration-encoded molecular communication,” *IEEE Trans. Nanobiosci.*, vol. 13, no. 3, pp. 208–222, Sep. 2014.
- [15] V. Jamali, A. Ahmadzadeh, C. Jardin, H. Sticht, and R. Schober, “Channel estimation for diffusive molecular communications,” *IEEE Trans. Commun.*, vol. 64, no. 10, pp. 4238–4252, Oct. 2016.
- [16] S. M. R. Rouzegar and U. Spagnolini, “Diffusive mimo molecular communications: Channel estimation, equalization, and detection,” *IEEE Trans. Commun.*, vol. 67, no. 7, pp. 4872–4884, Jul. 2019.
- [17] A. Noel, K. C. Cheung, and R. Schober, “Improving receiver performance of diffusive molecular communication with enzymes,” *IEEE Trans. NanoBiosci.*, vol. 13, no. 1, pp. 31–43, Mar. 2014.
- [18] —, “Using dimensional analysis to assess scalability and accuracy in molecular communication,” in *Proc. IEEE ICC Workshops 2013*, Budapest, Hungary, Jun. 2013, pp. 818–823.
- [19] —, “Bounds on distance estimation via diffusive molecular communication,” in *Proc. IEEE Globecom 2014*, Austin, TX, USA, Dec. 2014, pp. 2813–2819.
- [20] P. Cuatrecasas, “Membrane receptors,” *Annu. Rev. Biochem.*, vol. 43, no. 1, pp. 169–214, Jul. 1974.
- [21] H. B. Yilmaz, A. C. Heren, T. Tugcu, and C.-B. Chae, “Three-dimensional channel characteristics for molecular communications with an absorbing receiver,” *IEEE Commun. Lett.*, vol. 18, no. 6, pp. 929–932, Jun. 2014.

[22] M. Pierobon and I. F. Akyildiz, "Diffusion-based noise analysis for molecular communication in nanonetworks," *IEEE Trans. Signal Process.*, vol. 59, no. 6, pp. 2532–2547, Jun. 2011.

[23] A. S. Ladokhin, W. C. Wimley, and S. H. White, "Leakage of membrane vesicle contents: determination of mechanism using fluorescence requenching," *Biophys. J.*, vol. 69, no. 5, pp. 1964–1971, Nov. 1995.

[24] B. Alberts, D. Bray, K. Hopkin, A. D. Johnson, J. Lewis, M. Raff, K. Roberts, and P. Walter, *Essential Cell Biology*, 3rd ed. New York, NY, USA: Garland, 2010.

[25] M. Falk, J. Hüslér, and R.-D. Reiss, *Laws of Small Numbers: Extremes and Rare Events*. Springer, 2010.

[26] H. Pishro-Nik, *Introduction to Probability, Statistics, and Random Processes*. Kappa Research, LLC, 2016.

[27] D. Wackerly, W. Mendenhall, and R. L. Scheaffer, *Mathematical Statistics with Applications*. Pacific Grove, CA, USA: Duxbury, 2002.

[28] S. M. Kay, *Fundamentals of Statistical Signal Processing: Estimation Theory*. Upper Saddle River, NJ, USA: Prentice-Hall, 1993.

[29] E. L. Lehmann and G. Casella, *Theory of Point Estimation*. New York, NY: Springer-Verlag, 2006.

[30] M. J. Moore and T. Nakano, "Comparing transmission, propagation, and receiving options for nanomachines to measure distance by molecular communication," in *Proc. IEEE ICC 2012*, Ottawa, ON, Canada, Jun. 2012, pp. 6132–6136.

[31] J.-T. Huang, H.-Y. Lai, Y.-C. Lee, C.-H. Lee, and P.-C. Yeh, "Distance estimation in concentration-based molecular communications," in *Proc. IEEE Globecom 2013*, Atlanta, GA, USA, Dec. 2013, pp. 2587–2591.

[32] S. Liu, S. Bao, and C. Zhao, "Localization schemes for 2-D molecular communication via diffusion," in *Proc. CSPS 2019*, Apr. 2019, pp. 749–756.

[33] M. Turan, B. C. Akdeniz, M. S. Kuran, H. B. Yilmaz, I. Demirkol, A. E. Pusane, and T. Tugcu, "Transmitter localization in vessel-like diffusive channels using ring-shaped molecular receivers," *IEEE Commun. Lett.*, vol. 22, no. 12, pp. 2511–2514, Dec. 2018.

[34] Z. Luo, L. Lin, Q. Fu, and H. Yan, "An effective distance measurement method for molecular communication systems," in *Proc. IEEE SECON Workshops 2018*, Hong Kong, Jun. 2018, pp. 1–4.

[35] Y. Sun, M. Ito, and K. Sezaki, "An efficient distance measurement approach in diffusion-based molecular communication based on arrival time difference," in *Proc. ACM NanoCom 2017*, Washington DC, USA, Sep. 2017, pp. 1–6.

[36] S. Kumar, "Nanomachine localization in a diffusive molecular communication system," *IEEE Syst. J.*, vol. 14, no. 2, pp. 3011–3014, Jun. 2020.

[37] L. Lin, Z. Luo, L. Huang, C. Luo, Q. Wu, and H. Yan, "High-accuracy distance estimation for molecular communication systems via diffusion," *Nano Commun. Netw.*, vol. 19, pp. 47–53, Mar. 2019.

[38] S. Huang, L. Lin, W. Guo, H. Yan, J. Xu, and F. Liu, "Initial distance estimation and signal detection for diffusive mobile molecular communication," *IEEE Trans. Nanobiosci.*, vol. 19, no. 3, pp. 422–433, Jul. 2020.

[39] Y. Miao, W. Zhang, and X. Bao, "Cooperative source positioning for simo molecular communication via diffusion," in *Proc. IEEE ICCT 2019*, Xi'an, China, Oct. 2019, pp. 495–499.

[40] F. Gulec and B. Atakan, "Distance estimation methods for a practical macroscale molecular communication system," *Nano Commun. Netw.*, vol. 24, p. 100300, May 2020.

[41] R. Wang, *Introduction to Orthogonal Transforms: with Applications in Data Processing and Analysis*. Cambridge Univ. Press, Apr. 2012.

[42] H. Bruus, *Theoretical Microfluidics*, 1st ed. Oxford, U.K.: Oxford Univ. Press, 2007.

[43] W. Wicke, T. Schwering, A. Ahmadzadeh, V. Jamali, A. Noel, and R. Schober, "Modeling duct flow for molecular communication," in *Proc. IEEE Globecom 2018*, Abu Dhabi, United Arab Emirates, Dec. 2018, pp. 206–212.

[44] M. Schäfer, W. Wicke, L. Brand, R. Rabenstein, and R. Schober, "Transfer function models for cylindrical mc channels with diffusion and laminar flow," Jul. 2020. [Online]. Available: arXiv:2007.01799

[45] J. J. Moré, "The levenberg-marquardt algorithm: implementation and theory," *Numer. Anal.*, pp. 105–116, 1978.

[46] N. Farsad, W. Guo, and A. W. Eckford, "Tabletop molecular communication: Text messages through chemical signals," *PloS One*, vol. 8, no. 12, p. e82935, Dec. 2013.

[47] S. S. Andrews and D. Bray, "Stochastic simulation of chemical reactions with spatial resolution and single molecule detail," *Phys. Biol.*, vol. 1, no. 3, p. 137, Aug. 2004.

[48] A. Sadeghi, S. Ghavami, and G. B. Giannakis, "Performance bounds of estimators in molecular communications under structural constraints," in *Proc. ACM NanoCom 2017*, Sep. 2017, pp. 1–6.

[49] M. Schäfer, A. Ruderer, and R. Rabenstein, "An eigenfunction approach to parameter estimation for 1d diffusion problems," in *Proc. ECC 2019*, Jun. 2019, pp. 3784–3789.

[50] X. Huang, Y. Fang, A. Noel, and N. Yang, "Parameter estimation in a noisy 1D environment via two absorbing receivers," in *Proc. IEEE Globecom 2020*, Taipei, Taiwan, Dec. 2020.

[51] L. Lin, C. Yang, M. Ma, and S. Ma, "Diffusion-based clock synchronization for molecular communication under inverse gaussian distribution," *IEEE Sens. J.*, vol. 15, no. 9, pp. 4866–4874, Sep. 2015.

[52] S. K. Tiwari and P. K. Upadhyay, "Maximum likelihood estimation of snr for diffusion-based molecular communication," *IEEE Wireless Commun. Lett.*, vol. 5, no. 3, pp. 320–323, Jun. 2016.

[53] X. Huang, Y. Fang, A. Noel, and N. Yang, "Channel characterization for 1-D molecular communication with two absorbing receivers," *IEEE Commun. Lett.*, vol. 24, no. 6, pp. 1150–1154, Jun. 2020.

[54] H. S. S. A. Gelman, J. B. Carlin and D. B. Rubin, *Bayesian Data Analysis*. New York, NY, USA: Taylor & Francis, 2014.

[55] S. Abdallah and A. M. Darya, "Semi-blind channel estimation for diffusive molecular communication," *IEEE Commun. Lett.*, vol. 24, no. 11, pp. 2503–2507, Nov. 2020.

[56] A. Ahmadzadeh, H. Arjmandi, A. Burkowski, and R. Schober, "Comprehensive reactive receiver modeling for diffusive molecular communication systems: Reversible binding, molecule degradation, and finite number of receptors," *IEEE Trans. Nanobiosci.*, vol. 15, no. 7, pp. 713–727, Oct. 2016.

[57] H. Arjmandi, A. Ahmadzadeh, R. Schober, and M. N. Kenari, "Ion channel based bio-synthetic modulator for diffusive molecular communication," *IEEE Trans. Nanobiosci.*, vol. 15, no. 5, pp. 418–432, Jul. 2016.

[58] X. Huang, Y. Fang, A. Noel, and N. Yang, "Membrane fusion-based transmitter design for molecular communication systems," in *Proc. IEEE ICC 2021*, Montreal, Canada, Jun. 2021.

[59] D. T. McGuiness, S. Giannoukos, S. Taylor, and A. Marshall, "Experimental and analytical analysis of macro-scale molecular communications within closed boundaries," *IEEE Trans. Mol. Biol. Multi-Scale Commun.*, vol. 5, no. 1, pp. 44–55, Oct. 2019.

[60] L. Grebenstein, J. Kirchner, W. Wicke, A. Ahmadzadeh, V. Jamali, G. Fischer, R. Weigel, A. Burkowski, and R. Schober, "A molecular communication testbed based on proton pumping bacteria: Methods and data," *IEEE Trans. Mol. Biol. Multi-Scale Commun.*, vol. 5, no. 1, pp. 56–62, Oct. 2019.

[61] Y. Fang, A. Noel, N. Yang, A. W. Eckford, and R. A. Kennedy, "Symbol-by-symbol maximum likelihood detection for cooperative molecular communication," *IEEE Trans. Commun.*, vol. 67, no. 7, pp. 4885–4899, Jul. 2019.